



## Effect of Tribological and Electrochemical properties of AlTiN Coating by PVD (LARC) Technology for Medical Application

H. Sajjad<sup>1</sup>, M. U. Manzoor<sup>1\*</sup>, H. Zafar<sup>1</sup>, K. Shahzad<sup>2</sup>, F. Hussain<sup>1</sup>

Submitted: 27/01/2021, Accepted: 17/03/2021, Online: 26/03/2021

### Abstract

*Physical Vapor Deposition (PVD) technique is always an important technique to deposit metallic and ceramic coatings on different metallic substrates. The glow discharge process can be improved in a physical vapor deposition coating process by using at least two lateral rotating cathodes with targets. Lateral Arc Rotating Cathode (LARC) technology was used to deposit Aluminium titanium nitride (AlTiN) coating on stainless steel samples for biomedical implant application. The lateral rotation of cathode makes the uniform consumption of the cathodes in the coating chamber to get the maximum yield. The coating was characterized by Scanning Electron Microscopy (SEM) and Energy Dispersive X-ray Spectroscopy (EDX) for their uniformity and thickness. Open circuit potential (OCP), Electrochemical Impedance Spectroscopy (EIS) and Cyclic polarization test were performed for their corrosion behavior in ringer lactate solution. Tribological testing was also performed at three different loads to evaluate the coefficient of friction of the coating. The Electrochemical tests indicated that corrosion resistance of the coated sample was better than the uncoated substrate and it behaved like cathodically protected coating and showed more resistivity. The tribological test also showed improved coating quality with respect to the applied load.*

**Keywords:** Physical Vapor Deposition, LARC, AlTiN Coating, Corrosion Resistance, Electrochemical Impedance Spectroscopy, Scanning Electron Microscopy

### 1. Introduction:

Austenitic stainless steel SS316, Cobalt-Chromium (Co-Cr) alloy and Titanium alloys are the commonly used biomaterials in manufacturing of artificial implants and prosthesis because they offer tremendous biocompatibility, strength, corrosion resistance and mechanical properties in body environment [1-3]. In the previous years, about 10% of hip arthroplasties of stainless steel 316 must be changed due to local corrosion and fretting fatigue, which results from the high chloride ion concentration and modest temperature of human

body fluid [4, 5]. Therefore, to increase the life and working of biomaterials as an implant, surface treatments are necessary. For the surface treatments, introduction of corrosion resistant coatings on implants is one of the important aspects [6]. The addition of metallic component like aluminium in nitride coatings, introduces unique characteristics in coating like hardness, wear resistance at normal room temperature and at high temperature as well. The addition of aluminium in nitride based coatings make it more thermally stable, oxidation resistant with improved mechanical properties [7, 8].

<sup>1</sup>Institute of Metallurgy & Materials Engineering, Quaid-e-Azam Campus, University of the Punjab, Lahore, Pakistan

<sup>2</sup>Institute of Chemical Engineering & Technology, Quaid-e-Azam Campus, University of the Punjab, Lahore, Pakistan

**Corresponding Author:** [umar.imme@pu.edu.pk](mailto:umar.imme@pu.edu.pk)

Physical Vapor Deposition (PVD) is used to deposit thin hard coatings on a variety of substrates for numerous applications with basic principle of sputtering process in which target species are deposited on the substrate. The LARC technology has an added advantage over conventional PVD system that the cathodes are rotating giving uniform coating thickness, cathode erosion and higher degree of ionization [9, 10]. The metal ions from the cathode are accelerated towards the negatively biased substrate and deposited there [11, 12].

Aluminium titanium nitride (AlTiN) is a hard coating which is mostly used for the tribological properties. It can be coated on variety of ferrous and non-ferrous samples with a temperature range of 450-475 °C. A large ratio of aluminium in AlTiN coating makes it excellent oxidation and corrosion resistant with high hardness [13]. The protective nature of aluminium oxide [14] makes it suitable for biomedical application. The lamellar structure of Al rich AlTiN coating provides better wear resistant properties under dry condition and up to 900°C [15, 16]. The strength and toughness of the TiAlN coating is increased by the biomimetic self-assembly approach in which hard and tough sublayers developed during the coating process and each sublayer having complex lamellar hierarchy nanostructure is responsible for the improved mechanical properties [17].

Some researchers have worked on the adhesion, improved mechanical properties and compressive residual stress [18] of thin nano ceramic coating on different substrates for textile [19], biomedical implant [20, 21] among other various applications. Chung *et al.* [22] studied the TiAlN layer deposited as top layer to improve the biocompatibility of substrate Ni- Cr alloy for dental application by reactive radiofrequency sputtering techniques. The corrosion behavior of the Ni-Cr alloy was investigated by immersing the samples in Ringer Lactate solution for 24 hours and then implanted in guinea pigs for 12 weeks to study the biocompatibility of the tissue and the film. The results showed that corrosion behavior of the film

was improved. An austempered ductile iron was coated with TiAlN by Cheng Hsun Hsu *et al.* [23] using cathodic arc deposition to evaluate the erosion and corrosion resistance behavior. To evaluate the corrosion behavior, 3.5% NaCl immersion test was conducted. Passive aluminium oxide layer helped to improve the corrosion resistance. Qianzhi *et al.* [24] studied the electrochemical properties of different thin coatings on tungsten carbide (WC) discs. The coatings were developed by cathodic arc magnetron sputtering with both electrical and magnetic field. Four different coatings were evaluated for their corrosion resistance behavior in simulated body fluid. Out of them, TiAlN coating did not provide enough resistance due to hydration effect. Some researchers [25, 26] fabricated AlTiN coating using cathodic arc on plating technique on austenitic stainless steel, HSS. The coatings were not characterized for biocompatibility purpose but for machining.

Aluminium and titanium oxides formed on AlTiN film act as protective layer and make material oxidation/corrosion resistance and also provide better strength to substrate [27]. Also the titanium oxides provide lubricating effect while Aluminium oxide gives wear resistance and protects the coating at high temperature under load bearing application [28]. Fine grain nano-crystalline AlTiN coatings provide better strength to surface due to thick layer of alumina formed on surface, which makes it stable during wear mechanism [25, 29].

The study on electrochemical and tribological behavior of AlTiN coatings on stainless steel SS 316 for the purpose of biomedical implant application is very scarce. The current research is focused on tribo and corrosion evaluation of coating under different loading and immersion conditions.

## 2. Experimental Work:

The medical grade Austenitic Stainless steel 316 was cut into 1 cm<sup>2</sup> rectangular samples for electrochemical and surface characterization and 1-inch diameter disk with 5 mm thickness for tribological testing, by wire cutting. The chemical composition of Austenitic Stainless steel 316

purchased from the local market is shown in table 1.

**Table 1:** Chemical composition of SS 316

| Elements | % Composition |
|----------|---------------|
| Cr       | 18.00         |
| Ni       | 14.00         |
| Mo       | 3.00          |
| Mn       | 2.00          |
| Si       | 0.75          |
| C        | 0.08          |
| P        | 0.045         |
| S        | 0.03          |
| Fe       | Balance       |

The test samples were ground and polished according to ASTM E 3 standard. The grinding process was done as per FEPA grade on P100, P200, P400, P600, P800 and P1000 numbered SiC grinding papers. Polishing was done on velvet and nylon clothes using a diamond paste with particle size ranging from 6, 3, 1 and 0.25 mm on (*Ecomet 250 Grinder/Polisher USA*) automatic polisher to get surface roughness value less than 1 micron. The substrates were then coated with AlTiN thin film using Physical Vapor Deposition (PVD), Lateral Arc Rotating Cathodes (LARC) sputtering technology (*Platit 80 Switzerland*), the parameters have been described in another research work [30]. Scanning Electron Microscopy (SEM) with EDX (*Mira 3 TESCAN USA*) was used to determine the coating thickness and chemical composition of the coating and surface morphologies of samples before and after corrosion testing. The corrosion behavior of the coated and uncoated samples was studied in Ringer lactate solution. The chemical composition of Ringer lactate solution is shown in table 2.

**Table 2:** Composition of ringer lactate solution

| Composition   | g/L |
|---|-----|
| NaCl  | 6.0 |
| KCl   | 0.4 |
| CaCl <sub>2</sub> (H <sub>2</sub> O)                      | 0.3 |
| C <sub>3</sub> H <sub>5</sub> NaO <sub>3</sub> (50% sol.) | 6.1 |
| HCl (25% sol.)  | 0.2 |

Open circuit potential (OCP), Electrochemical

Impedance Spectroscopy (EIS) and Cyclic polarization was carried out using Potentiostat (*GAMRY interface 3000 USA*) with different exposure time. A three-electrode system consisting of a reference (saturated calomel electrode (SCE)), a counter electrode (pure platinum sheet) and the working electrode (coated sample) was used. Open circuit potential was carried out after 1-day exposure time in ringer lactate for 500 sec. Electrochemical Impedance Spectroscopy was performed at 10 mV<sub>rms</sub> w.r.t OCP, AC potential amplitude within 100 kHz – 10 MHz frequency range. Cyclic polarization was done at initial voltage of -0.5V vs. Eoc, forward scan 5mV/s, and reverse scan 2.5mV/s. The OCP and EIS were again performed after exposure time of 20 days and 40 days. The friction behavior of AlTiN coated SS316 substrates was characterized by ball on disc Tribometer (*CSM Instruments SA Switzerland*). The static medium was hard Al<sub>2</sub>O<sub>3</sub> ball having 6 mm radius. Tribo tests were carried out with 1N, 2N, 3N respectively, with linear speed of 20cm/sec under lubricated (ringer lactate as lubricating media) and dry condition. Friction coefficient and penetration depths were recorded.

### 3. Results & Discussion:

#### 3.1 Surface Characterization:

SEM image of AlTiN coated on SS316 interface is shown in figure 1, which reveals AlTiN coating having average thickness of 2.58 μm.

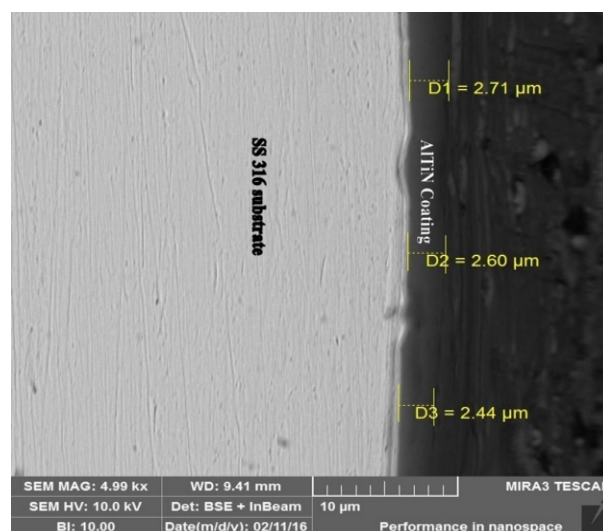


**Figure 1:** SEM image AlTiN coated on SS316 interface

An EDX spectra showing chemical composition of aluminium and titanium coating from interface is shown in figure 2.

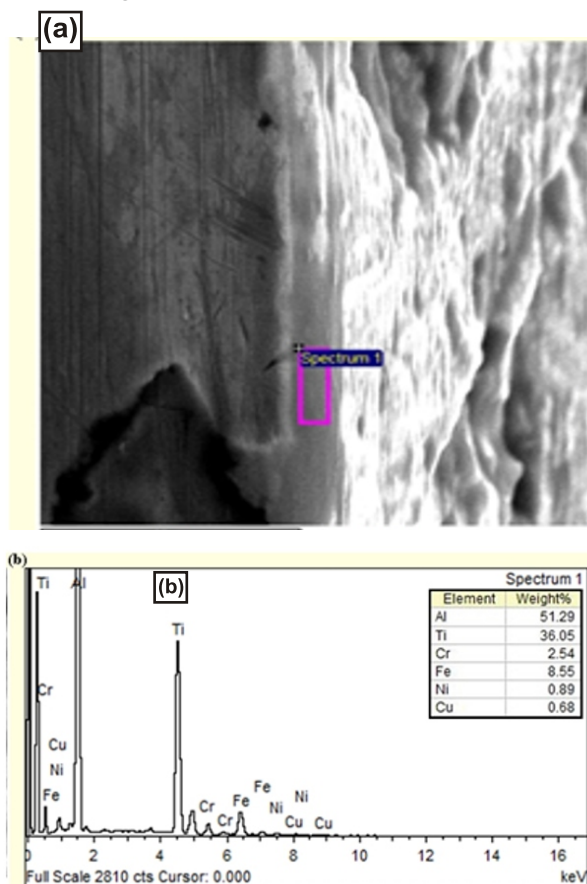


**Figure 2:** (a) SEM Image of AlTiN coated interface, (b) EDX spectra of interface

### 3.2 Electrochemical Analysis:

#### 3.2.1 Open Circuit Potential:

The open circuit potential (OCP) w.r.t to SCE of SS316 and AlTiN coated on SS316 is shown in figure 3. After exposure of 1 day in ringer lactate, open circuit potential (OCP) of SS316 and AlTiN coating on SS316 is -295.4 mV and -204.1 mV respectively. The OCP of AlTiN coated substrate is noble in comparison with SS316 substrate. After 20 days of exposure, open circuit potential of SS316 and AlTiN coated on SS316 is -141.84 mV and -155.7 mV respectively. The open circuit potential (OCP) values for SS316 after 40 days is 146.6 mV and for AlTiN coated SS316 it is -0.1406V. From this trend it can be said that as exposure time in ringer

lactate increases, open circuit potential of SS316 is shifted towards noble side as compared to AlTiN coating on SS316 which depicts that SS316's behavior in Ringer solution is passive than that of the coated Ss316.

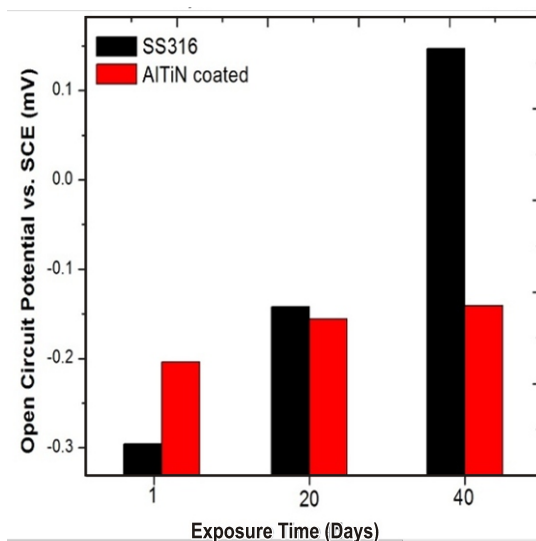


**Figure 3:** Open circuit potential for SS316 and AlTiN coated on SS316.

#### 3.2.2 Electrochemical Impedance Spectroscopy (EIS):

The Nyquist plot of SS316 substrate and AlTiN coating on SS316 for 1 day, 20 days and 40 days' immersion in ringer lactate solution respectively is shown in figure 4. From figure 4, it is indicated that after 1 day of immersion, AlTiN coating on SS316 showed more resistance than that of SS316. The polarization resistance for SS316 and AlTiN coated on SS316 is 22.96 k .cm<sup>2</sup> and 105.17k .cm<sup>2</sup> respectively. It can also be observed that complete loop is not formed which is an indication of non-ideal capacitive behavior of substrates in an electrolyte solution. After 20 days, there is an intimate contact of substrates with an electrolyte, the resistance of AlTiN coated on SS316 is decreased abruptly even its polarization resistance (2.40 k .cm<sup>2</sup>) drops down from the SS316 polarization resistance (19.94 k .cm<sup>2</sup>). An abrupt change in polarization resistance is also noted because, as the time of immersion increases, the compactness of AlTiN coating is disturbed. The polarization resistance for AlTiN coated substrate is 1.260 k .cm<sup>2</sup> and that of SS316 is 16.17 k .cm<sup>2</sup>.

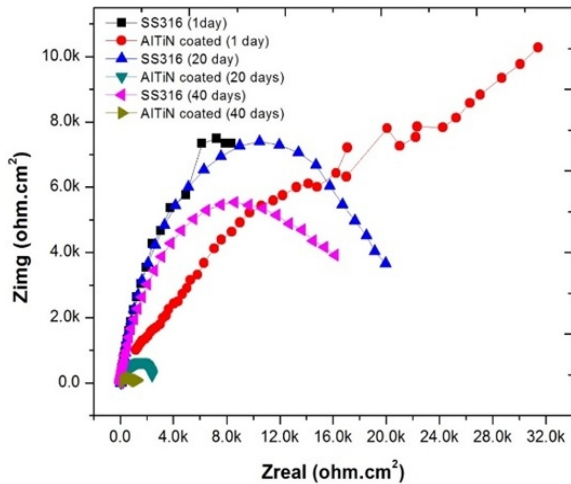


**Figure 4:** Nyquist plot of SS316 and AlTiN coated on SS316.

Equivalent circuit diagram of electrochemical behavior of coating is presented in figure 5. R.E represents the Reference Electrode.  $R_u$  being an uncompensated resistance (which is usually resistance of electrolyte at interface),  $Y_o$  represent constant phase which is indication of non-ideal capacitive behavior as shown in Nyquist plot in figure 4. R1 and R2 represent resistances of AlTiN coated SS316 and SS316 capacitive circuit. Whereas W.E represents the working electrode.

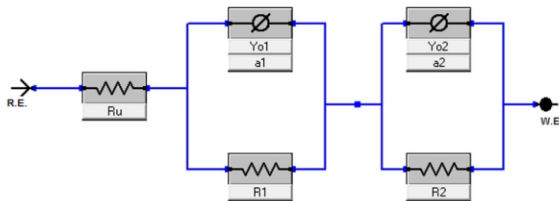


**Figure 5:** Equivalent circuit diagram of AlTiN coated SS316.

After electrochemical impedance spectroscopy of AlTiN coated on SS316 and SS316 surfaces, fig 6 (a, b) shows the scanning electron microscopy of the surfaces. Figure 6a shows white layers on SS316 surface which is because of salt formation during a contact with ringer lactate solution [30]. The salt formation process reduces the resistance of substrate. Figure 6b reveals coating morphology after electrochemical testing. Pits and holes are observed on AlTiN coated on SS316. The porosity in coating layer is stated as main reason of reduction in the corrosion resistance of AlTiN coated substrate after immersion in Ringer lactate solution. AlTiN coating has improved oxidation and corrosion resistance properties as compared to TiN, because  $Al_2O_3$  and  $TiO_2$  act as barrier for corrosion elements to damage both the coating and the substrate [29, 31, 32]. PVD coatings possess high density and strong adhesion. However, the macro defects such as inclusions and voids formed due to the micro-metal droplets, emitted from the cathodes, reduce the corrosion resistance of the coatings. In many applications, the coated parts are frequently exposed to an aggressive working environment. For instance, a chloride containing corrosive medium, particularly in a marine region, is promoting localized corrosion due to the strong effect of Cl<sup>-</sup> ions [33]. These porosity defects in the AlTiN coating, originating from the deposition of the coatings, acted as pathways for Chloride ions to penetrate through the coatings and attack the steel substrate [34].

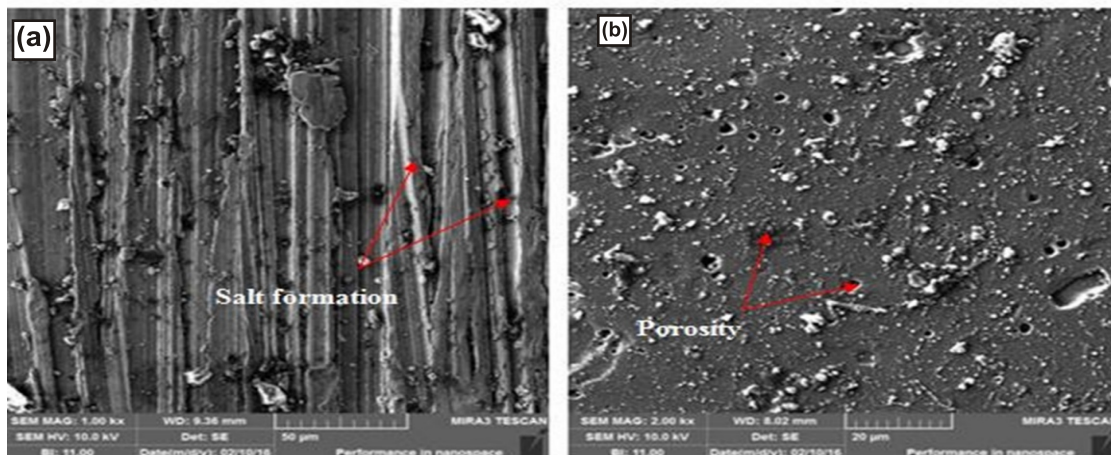


**Figure 6:** Scanning Electron Microscopy of (a) uncoated substrate and (b) AlTiN coated substrate

Energy Dispersive X-Ray spectra and chemical composition of coating after electrochemical testing is given in figure 7.

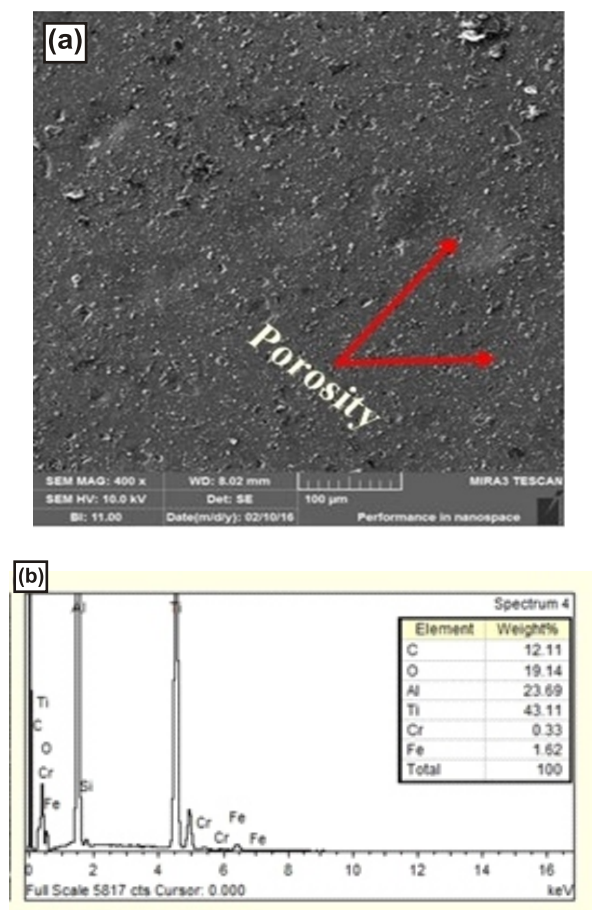


**Figure 7:** EDX analysis of AlTiN coated on SS 316 specimen after electrochemical testing

From the above spectra it is indicated that Al content of AlTiN coating has decreased from 51.29 wt. % to 23.69 wt. %. So it can be said that Aluminium has been removed and leaving behind the porosity in the coating layer and decreasing its corrosion resistance.

### 3.2.3 Cyclic Polarization:

The cyclic polarization of SS316 and AlTiN coated on SS316 was carried out after immersion in ringer lactate for 12 hours. In figure 7, polarization curves for both substrates are given. From figure 7, it can be seen that for SS316, negative loop is completed in cyclic curve which is indication of no pitting. Whereas for AlTiN coated on SS316 positive loop is completed and a small hysteresis loop was formed

which indicates that pits are produced on coated surface. The loop size can be interpreted with the extent of pitting [35-37]. These results are supporting the electrochemical impedance spectroscopy (EIS) results of AlTiN coated on SS316 which stated that coating resistance abruptly decreases as immersion time increases.  $I_{corr}$  of SS316 is  $14.20 \times 10^{-9}$  A.cm<sup>-2</sup> and AlTiN coated on SS316 is  $1.75 \times 10^{-6}$  A.cm<sup>-2</sup> calculated by tafel extrapolation method. In corrosive environment, low current density shows that material is corrosion resistant. Corrosion rates of SS 316 and AlTiN coated on SS 316 are  $6.11 \times 10^{-3}$  mpy and  $750.6 \times 10^{-3}$  mpy respectively.

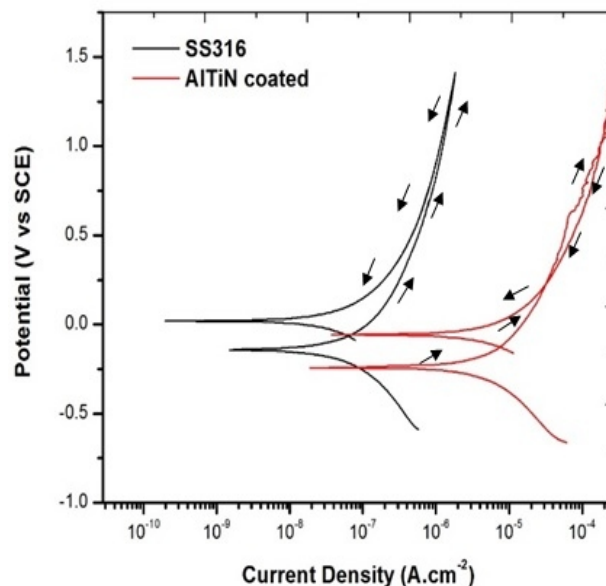


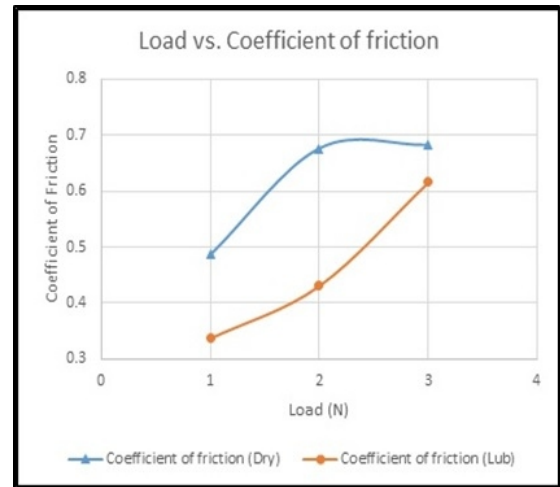
**Figure 8:** Cyclic polarization curve for SS316 and AlTiN coated on SS316

### 3.3 Tribological Evaluation of AlTiN coating:

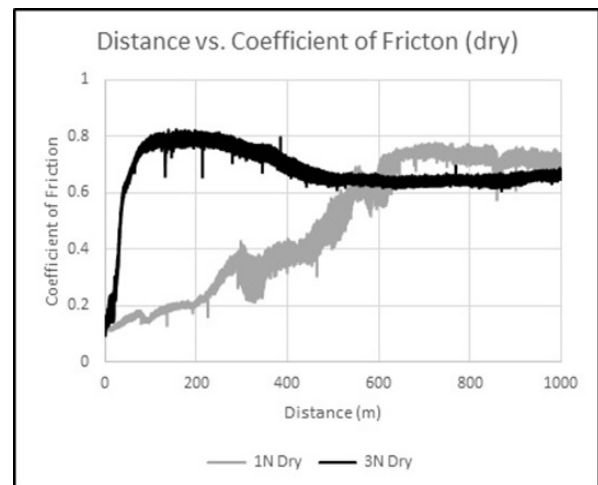
The tribological evaluation is carried out at three different loads with constant linear speed of 20cm/sec. Ringer lactate was used as a lubrication medium for the tribological test. The graph between the average coefficient of friction of coating under dry and lubricating condition at three different loads is shown in figure 9. The tribo test curves in dry and lubricating media at different loading conditions are given in figure 10 and 11 respectively.

Figure 9 shows the graphical representation of

coefficient of friction of coated samples with different loads under dry and lubricated conditions. Figure shows the clear difference in coefficient of friction under both conditions. Coated samples in dry conditions exhibit high coefficient of friction values as compared to that of samples operated in lubricating conditions, which is expected because as the load increases, the coefficient of friction values also increases. Under dry conditions, it can be seen that the value of coefficient of friction is increased by 28% as we increase the load from 1N to 2N. But there is no vital change in coefficient of friction value from 2N load to 3N. This is due to the fact that at low load, the friction between the mating surfaces is low and the coating is bearing the load of 1N. the graph shown in figure 10, is also indicating that initially the coefficient of friction value is increasing with the distance covered but after 600 m the coefficient of friction is stable. But when the load increases, the average coefficient of friction value also increases and graph in the figure 10 indicates high coefficient of friction up to a distance of 100 m and then a stable value till the end of the test. The stable value of coefficient of friction under 1N and 3N load indicates that the coating is still intact even at a load of 3N under dry condition. While under lubricating conditions, the coefficient of friction value is increasing with the load but at all the three loads, it is still lower than the dry condition. It can be seen from figure 11, that the coefficient of friction values are increasing with load which is in good relation with the average coefficient of friction values shown in figure 9. At start of the test, there is a sudden increase of the coefficient of friction values but after covering a distance of approximately 100 m, the curves are near to linearity. This trend is because of the lubrication medium which is keeping the surfaces safe. There is slight deviation of linearity in the curve at different distances which is due to the amount of lubrication getting in and out of the track of the ball during the test [28, 38-41].



**Figure 9:** Coefficient of Friction of coating at different loading curves under dry and lubricating conditions



**Figure 10:** Friction behavior of AlTiN coated substrate in dry environment.

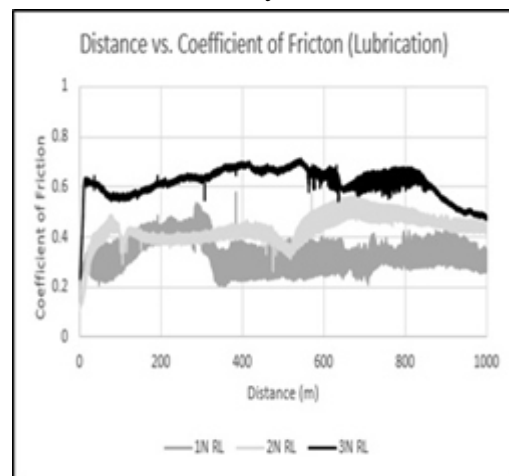


**Figure 11:** Friction behavior of AlTiN coated substrate in Ringer lactate.

### Conclusion:

AlTiN coating is deposited on Stainless steel grade 316 substrate by Physical Vapor Deposition process using LARC technology to assess the electrochemical and tribological compatibility of coating in Ringer lactate solution. Coating thickness was observed as 2.58 microns. Electrochemical characterization revealed that AlTiN coating exhibited low resistance for longer duration in the ringer lactate solution, the coating loses its compactness and chemical composition after immersion in artificial body fluid. The tribological results show that with the increase of load up to 3N, the coefficient of friction first increases and then stable with the line of low load of 1N. Similarly, under lubricating conditions, high load shows high coefficient of friction than that of low load samples.

### Acknowledgment:

The authors would like to thank the PITMAEM, PCSIR Labs Complex, Lahore for providing the necessary arrangement for coating and also to The University of the Punjab Lahore for providing necessary financial supports in completing this research.

### References:

1. S. Hosseinalipour, A. Ershad-Langroudi, A. N. Hayati, and A. Nabizade-Haghighi, "Characterization of solgel coated 316L stainless steel for biomedical applications," *Progress in Organic Coatings*, vol. 67, pp. 371-374, 2010.
2. J. Pellier, J. Geringer, and B. Forest, "Fretting-corrosion between 316L SS and PMMA: Influence of ionic strength, protein and electrochemical conditions on material wear. Application to orthopaedic implants," *Wear*, vol. 271, pp. 1563-1571, 2011.
3. F. Yýldýz, A. Yetim, A. Alsaran, A. Celik, and I. Kaymaz, "Fretting fatigue properties of plasma nitrided AISI 316 L stainless steel: experiments and finite element analysis," *Tribology International*, vol. 44, pp. 1979-1986, 2011.
4. K. Nielsen, "Corrosion of metallic implants," *British Corrosion Journal*, vol. 22, pp. 272-278, 1987.
5. S. A. Brown and K. Merritt, "Fretting corrosion in saline and serum," *Journal of biomedical materials research*, vol. 15, pp. 479-488, 1981.
6. I. Pohrelyuk, V. Fedirko, O. Tkachuk, and R. Proskurnyak, "Corrosion resistance of Ti6Al4V alloy with nitride coatings in Ringer's solution," *Corrosion science*, vol. 66, pp. 392-398, 2013.
7. T. Cselle, O. Coddet, C. Galamand, P. Holubar, M. Jilek, J. Jilek, *et al.*, "Triplecoatings3®-New generation of PVD-Coatings for cutting tools," *Journal of machine manufacturing*, vol. 49, pp. 19-25, 2009.
8. Y.-p. Feng, L. Zhang, R.-x. Ke, Q.-l. Wan, Z. Wang, and Z.-h. Lu, "Thermal stability and oxidation behavior of AlTiN, AlCrN and AlCrSiWN coatings," *International Journal of Refractory Metals and Hard Materials*, vol. 43, pp. 241-249, 2014.
9. K. J. A. Brookes and A. Lmkemann, "PLATIT pioneers in physical vapour deposition," *Metal Powder Report*, vol. 68, pp. 24-27, 2013/03/01/ 2013.
10. L. Krzysztof, "- Review of Nanocomposite Thin Films and Coatings Deposited by PVD and CVD Technology N2 - The book pp. - Ch. 7.
11. (2021). [www.platit.com](http://www.platit.com). Available: [www.platit.com](http://www.platit.com)
12. Ť. A. V. P. P. DEPONOVANÝCH, "Structure and properties of PVD coatings deposited by ARC and LARC technology," *Acta Metallurgica Slovaca*, vol. 15, pp. 221-227, 2009.
13. Y. - Y. Chang and D. - Y. Wang, "Characterization of nanocrystalline AlTiN coatings synthesized by a cathodic-arc deposition process," *Surface and Coatings Technology*, vol. 201, pp. 6699-6701, 2007.
14. E. Denes, G. Barrire, E. Poli, and G. Lvque,

- "Alumina Biocompatibility," *J Long Term Eff Med Implants*, vol. 28, pp. 9-13, 2018.
15. "<https://robbjack.com/support-article/altin-coated-carbide-coating/>," 2019.
  16. J. Todt, J. Zalesak, R. Daniel, R. Pitonak, A. Köpf, R. Weißenbacher, *et al.*, "Al-rich cubic Al<sub>0.8</sub>Ti<sub>0.2</sub>N coating with self-organized nanolamellar microstructure: Thermal and mechanical properties," *Surface and Coatings Technology*, vol. 291, pp. 89-93, 2016/04/15/2016.
  17. M. Meindlhumer, J. Zalesak, R. Pitonak, J. Todt, B. Sartory, M. Burghammer, *et al.*, "Biomimetic hard and tough nanoceramic TiAlN film with self-assembled six-level hierarchy," *Nanoscale*, vol. 11, pp. 7986-7995, 2019.
  18. M. Renzelli, M. Z. Mughal, M. Sebastiani, and E. Bemporad, "Design, fabrication and characterization of multilayer Cr-CrN thin coatings with tailored residual stress profiles," *Materials & Design*, vol. 112, pp. 162-171, 2016/12/15/2016.
  19. S. Alam, M. Irfan, B. D. Soomro, M. Shahid, and M. Zeeshan, "Optimization of loading factor of Nanocomposite Coatings deposited by Physical Vapor Deposition," *Journal of Physics: Conference Series*, vol. 439, p. 012016, 2013/06/10 2013.
  20. G. M. Uddin, M. Jawad, M. Ghufran, M. W. Saleem, M. A. Raza, Z. U. Rehman, *et al.*, "Experimental investigation of tribomechanical and chemical properties of TiN PVD coating on titanium substrate for biomedical implants manufacturing," *The International Journal of Advanced Manufacturing Technology*, vol. 102, pp. 1391-1404, 2019/06/01 2019.
  21. G. M. Uddin, M. Sajid Kamran, J. Ahmad, M. Ghufran, M. Asim, M. Qasim Zafar, *et al.*, "Comparative Experimental Study of Tribomechanical Performance of Low-Temperature PVD Based TiN Coated PRCL Systems for Diesel Engine," *Advances in Tribology*, vol. 2018, p. 9437815, 2018/12/12 2018.
  22. K. Chung, G. Liu, J. Duh, and J. Wang, "Biocompatibility of a titaniumaluminum nitride film coating on a dental alloy," *Surface and Coatings Technology*, vol. 188, pp. 745-749, 2004.
  23. C. H. Hsu, J. K. Lu, and M. L. Chen, "Study on Characteristics of ADI Coated DLC/TiN/TiAlN Coatings by Cathodic Arc Evaporation," in *Solid State Phenomena*, 2006, pp. 257-264.
  24. Q. Wang, F. Zhou, C. Wang, M.-F. Yuen, M. Wang, T. Qian, *et al.*, "Comparison of tribological and electrochemical properties of TiN, CrN, TiAlN and aC: H coatings in simulated body fluid," *Materials Chemistry and Physics*, vol. 158, pp. 74-81, 2015.
  25. J. Endrino, G. Fox-Rabinovich, and C. Gey, "Hard AlTiN, AlCrN PVD coatings for machining of austenitic stainless steel," *Surface and Coatings Technology*, vol. 200, pp. 6840-6845, 2006.
  26. J. Vetter, O. Kayser, and H. W. Bieler, "AlTiNa universal coating for different applications: from dry cutting to decoration. AlTiN Die Universal-Beschichtung für eine Vielzahl von Anwendungen: von Trockenzerspannung bis Dekor," *Vakuum in Forschung und Praxis*, vol. 17, pp. 131-134, 2005.
  27. H. C. Barshilia, "Growth, characterization and performance evaluation of Ti/AlTiN/AlTiON/AlTiO high temperature spectrally selective coatings for solar thermal power applications," *Solar Energy Materials and Solar Cells*, vol. 130, pp. 322-330, 2014.
  28. M. Szala, M. Walczak, K. Pasierbiewicz, and M. Kamiński, "Cavitation Erosion and Sliding Wear Mechanisms of AlTiN and TiAlN Films Deposited on Stainless Steel Substrate," *Coatings*, vol. 9, p. 340, 2019.
  29. K. Dejun and F. Guizhong, "Friction and wear behaviors of AlTiCrN coatings by cathodic arc ion plating at high temperatures," *Journal of Materials Research*, vol. 30, pp. 503-511, 2015/02/01 2015.

30. M. U. Manzoor, A. Salman, H. Sajjad, A. Farooq, T. Ahmad, M. Kamran, H. Zafar, F. Hussain, F. Riaz, "Electrochemical Characterization of AlTiN Coating on Stainless Steel Substrate for Biomedical Implant," *Journal of Pakistan Institute of Chemical Engineers*, vol. 48, 2021.
31. K. Dejun and G. Haoyuan, "Friction-wear behaviors of cathodic arc ion plating AlTiN coatings at high temperatures," *Tribology international*, vol. 88, pp. 31-39, 2015.
32. Q.-X. Fan, T.-G. Wang, Y.-M. Liu, Z.-H. Wu, T. Zhang, T. Li, *et al.*, "Microstructure and Corrosion Resistance of the AlTiN Coating Deposited by Arc Ion Plating," *Acta Metallurgica Sinica (English Letters)*, vol. 29, pp. 1119-1126, 2016/12/01 2016.
33. X.-z. Ding, A. L. K. Tan, X. T. Zeng, C. Wang, T. Yue, and C. Q. Sun, "Corrosion resistance of CrAlN and TiAlN coatings deposited by lateral rotating cathode arc," *Thin Solid Films*, vol. 516, pp. 5716-5720, 2008/06/30/ 2008.
34. M. S. Ahmed, P. Munroe, Z.-T. Jiang, X. Zhao, W. Rickard, Z.-f. Zhou, *et al.*, "Corrosion behaviour of nanocomposite TiSiN coatings on steel substrates," *Corrosion Science*, vol. 53, pp. 3678-3687, 2011/11/01/ 2011.
35. N. B. Huang, H. Yu, L. S. Xu, S. Zhan, M. Sun, and D. W. Kirk, "Corrosion kinetics of 316L stainless steel bipolar plate with chromiumcarbide coating in simulated PEMFC cathodic environment," *Results in Physics*, vol. 6, pp. 730-736, 2016/01/01/ 2016.
36. F. R. Foulkes and P. McGrath, "A rapid cyclic voltammetric method for studying cement factors affecting the corrosion of reinforced concrete," *Cement and Concrete Research*, vol. 29, pp. 873-883, 1999.
37. L. D'Avico, R. Beltrami, N. Lecis, and S. P. Trasatti, "Corrosion behavior and surface properties of PVD coatings for mold technology applications," *Coatings*, vol. 9, p. 7, 2019.
38. D. Özkan, Y. Erarslan, E. Sulukan, L. Kara, M. Alper Yılmaz, and M. B. Yađcý, "Tribological Behavior of TiAlN, AlTiN, and AlCrN Coatings at Boundary Lubricating Condition," *Tribology Letters*, vol. 66, p. 152, 2018/11/02 2018.
39. Q. He, J. M. DePaiva, J. Kohlscheen, B. D. Beake, and S. C. Veldhuis, "Study of wear performance and tribological characterization of AlTiN PVD coatings with different Al/Ti ratios during ultra-high speed turning of stainless steel 304," *International Journal of Refractory Metals and Hard Materials*, vol. 96, p. 105488, 2021/04/01/ 2021.
40. G. M. Uddin, A. A. Khan, M. Ghufran, Z.-u.-R. Tahir, M. Asim, M. Sagheer, *et al.*, "Experimental study of tribological and mechanical properties of TiN coating on AISI 52100 bearing steel," *Advances in Mechanical Engineering*, vol. 10, p. 1687814018802882, 2018.
41. W. H. Kao, Y. L. Su, J. H. Horng, and Y. T. Hsieh, "Improved tribological properties, electrochemical resistance and biocompatibility of AISI 316L stainless steel through duplex plasma nitriding and TiN coating treatment," *J Biomater Appl*, vol. 32, pp. 12-27, Jul 2017.